Cell

Type II Cadherin Ectodomain Structures: Implications for Classical Cadherin Specificity

Saurabh D. Patel,[1,5] Carlo Ciatto,[1,5] Chien Peter Chen,[1,5] Fabiana Bahna,[1,5] Manisha Rajebhosale,[3,5] Natalie Arkus,[1] Ira Schieren,[2] Thomas M. Jessell,[1,2] Barry Honig,[1,2] Stephen R. Price,[3,*] and Lawrence Shapiro[1,4,*]

[1] Department of Biochemistry and Molecular Biophysics, Columbia University, New York, NY 10032, USA
[2] Howard Hughes Medical Institute, Columbia University, New York, NY 10032, USA
[3] Department of Anatomy and Developmental Biology, University College, Gower Street, London WC1E 6bT, UK
[4] Edward S. Harkness Eye Institute, Columbia University, New York, NY 10032, USA
[5] These authors contributed equally to this work.
*Contact: ucgaspr@ucl.ac.uk (S.R.P.); lss8@columbia.edu (L.S.)
DOI 10.1016/j.cell.2005.12.046

SUMMARY

Type I and II classical cadherins help to determine the adhesive specificities of animal cells. Crystal-structure determination of ectodomain regions from three type II cadherins reveals adhesive dimers formed by exchange of N-terminal β strands between partner extracellular cadherin-1 (EC1) domains. These interfaces have two conserved tryptophan side chains that anchor each swapped strand, compared with one in type I cadherins, and include large hydrophobic regions unique to type II interfaces. The EC1 domains of type I and type II cadherins appear to encode cell adhesive specificity in vitro. Moreover, perturbation of motor neuron segregation with chimeric cadherins depends on EC1 domain identity, suggesting that this region, which includes the structurally defined adhesive interface, encodes type II cadherin functional specificity in vivo.

INTRODUCTION

Cadherins form a large family of transmembrane proteins that mediate calcium-dependent adhesive interactions between animal cells (Hatta and Takeichi, 1986; Nollet et al., 2000; Takeichi et al., 1981). The specificity of intercellular recognition conferred by cadherins has a critical role in the patterning of multicellular structures (Redies and Takeichi, 1996). Most of the morphogenetic functions of vertebrate cadherins have been ascribed to the "classical" cadherins, which comprise two major subfamilies, termed type I and type II cadherins (Nollet et al., 2000). Type I cadherins typically have broad distributions that are segregated by embryonic germ layer or tissue type (Nishimura et al., 1999). In contrast, type II cadherins exhibit more fine-grained, and often overlapping, patterns of expression, notably within the developing nervous system (Bekirov et al., 2002; Price et al., 2002).

Insights into the molecular basis of cadherin binding and specificity have emerged from atomic-resolution structural studies of type I cadherins. The type I cadherins possess an amino-terminal cell-surface-exposed region composed of tandemly repeated "extracellular cadherin" (EC) domains, EC1–EC5. Each of the type I cadherin structures resolved to date exhibits a dimer interface involving the exchange, or swapping, of a β strand between the partner cadherin EC1 domains (Boggon et al., 2002; Haussinger et al., 2004; Shapiro et al., 1995a). This swapping interaction is anchored by the insertion of the side chain of the conserved Trp2 residue into a complementary hydrophobic pocket in the partner molecule (Shapiro et al., 1995a). This interface has been proposed to mediate binding between cadherins presented from opposing cells. The symmetry of this interaction ensures that each cadherin-cadherin interface buries two Trp2 side chains, one from each protomer (Boggon et al., 2002). The strand exchange observed in cadherins exemplifies a more general domain-swapping strategy, which may enable homophilic interactions with low affinity yet high specificity (Chen et al., 2005).

Several lines of evidence support the idea that the amino-terminal EC1 domain functions in adhesive binding and specificity (for review, see Patel et al., 2003; Troyanovsky, 2005), but other results have led to proposals that multiple EC domains may be involved in cadherin binding (Chappuis-Flament et al., 2001; Perret et al., 2004; Sivasankar et al., 1999; Zhu et al., 2003). Thus, there is uncertainty as to whether cadherin-mediated adhesion depends solely on interactions of partner EC1 domains or on interdigitated EC domains.

The logic that governs the specificity of cadherin-based recognition remains enigmatic. In part, this reflects the

difficulty in assaying cadherin specificity under conditions that mimic those in vivo. For example, measurements of the adhesion of cells expressing type I cadherins to inert cadherin-coated substrates have revealed little specificity (Chappuis-Flament et al., 2001). Many cell-aggregation experiments have also revealed minimal specificity among cells expressing different type I cadherins (Duguay et al., 2003; Foty and Steinberg, 2005). Other in vitro cell-sorting assays, however, have provided evidence for differential specificity of type I cadherins, notably for cells that express combinations of E-, N-, and P-cadherins (Nose et al., 1990; Shan et al., 1999, 2000). These divergent findings may arise, in part, from sensitivity to cadherin expression level (Duguay et al., 2003; Foty and Steinberg, 2005) and could also reflect differences in intercellular forces obtained in vivo and in vitro.

In vitro aggregation assays with cells expressing type II cadherins have failed to reveal clear adhesive preferences (Shimoyama et al., 2000). Certain in vivo assays of type II cadherin interactions have, however, provided evidence for subtype specificity (Espeseth et al., 1998; Price et al., 2002). One system in which specificity has been demonstrated involves the segregation of distinct classes of motor neurons into discrete clusters, termed motor pools. In this in vivo context, different type II cadherins can exert distinct activities in the control of motor pool segregation (Price et al., 2002), supporting the existence of functional differences in the interactions of type II cadherins. But it remains unclear whether and how these differences emerge from the adhesive preferences of individual cadherin molecules.

Here, we present crystal structures of ectodomain regions from three type II cadherins: MN-cadherin, cadherin-8, and cadherin-11. Each reveals a dimeric configuration topologically similar to the strand-exchanged interfaces observed for type I cadherins, with adhesive interactions confined to the EC1 domains. However, the structural features of type II cadherins suggest that members of this family are not compatible as binding partners for type I family members. Our findings reveal that the EC1 domain of type II cadherins, which encodes the adhesive interface identified crystallographically, is a dominant element in determining functional specificity in vivo. Together with the structural features of type II cadherins revealed here, these findings begin to provide a mechanistic basis for the adhesive interaction of these proteins in vivo.

RESULTS

To define the basis of type II cadherin-mediated recognition, we determined the three-dimensional structures of five different fragments from type II cadherin ectodomains by X-ray crystallography. We focused on regions containing the N-terminal EC1 domain because prior structural (Boggon et al., 2002; Haussinger et al., 2004; He et al., 2003) and functional (Nose et al., 1990; Shan et al., 1999, 2000; Tamura et al., 1998; Troyanovsky et al., 2003) studies on type I cadherins showed that adhesion is mediated through EC1 domains and because some of the sequence elements required for type I cadherin adhesive binding are conserved in type II cadherins.

Structures of Multidomain Fragments from Type II Cadherins Show Dimers Formed through the EC1 Domain

The 3.2 Å resolution structure of a two-domain EC1-EC2 fragment from cadherin-11 is shown in Figure 1A. The overall structure is similar to that of corresponding regions from type I cadherins (Boggon et al., 2002; Nagar et al., 1996; Overduin et al., 1995; Shapiro et al., 1995a, 1995b), comprising two Greek-key-topology β sandwich domains, EC1 and EC2, joined by an interdomain calcium binding region that coordinates three Ca^{2+} ions (Figure 1A). The EC2 domain has a fold identical to that seen in type I cadherin structures. However, the type II EC1 domain differs from the type I EC1 domain in the absence of the region previously referred to as a pseudo-β helix between the C and D strands (Shapiro et al., 1995b). Primary-sequence elements of this region are conserved in all type I cadherins but absent from type II cadherins. The calcium ligands in the cadherin-11 structure (Figure 1B) are identical to those of type I cadherins (Nagar et al., 1996).

Cadherin-11 EC1-EC2 crystals have a single molecule in the crystallographic asymmetric unit, but a 2-fold symmetric dimer is observed between pairs of symmetry-related protomers. As in type I cadherins, each interacting protomer in a dimer complex exchanges its own A strand for that of its partner (Figure 1C). As can be seen in Figure 1C, the dimer interface in cadherin-11 consists solely of interactions involving the EC1 domain. Similar to the C-cadherin structure (Boggon et al., 2002), the EC1-EC2 dimer structure of cadherin-11 presented here provides further evidence that cadherin adhesive interactions are encoded in the EC1 domain and argues against the view that multiple cadherin domains are intercalated (Chappuis-Flament et al., 2001; Sivasankar et al., 1999; Zhu et al., 2003).

We also determined the structure of an EC1–EC3 ectodomain fragment from cadherin-8 (Figure 1D). Crystals of this molecule gave highly anisotropic diffraction patterns. Nonetheless, the structure was solved by molecular replacement, and we used anomalous diffraction from selenomethionine-labeled crystals to verify the structure. This anisotropic low-resolution (~4.5 Å/5.5 Å) structure also shows an adhesive interface mediated exclusively through EC1 domains, further underscoring the role of the EC1 domains in mediating adhesion.

Structures of EC1 Domains from MN-Cadherin, Cadherin-8, and Cadherin-11: Details of Adhesive Interface

To define structural features common to type II cadherins, and to address questions of binding specificity, we determined crystal structures of EC1 domains from cadherin-11, cadherin-8, and MN-cadherin. These EC1 domain

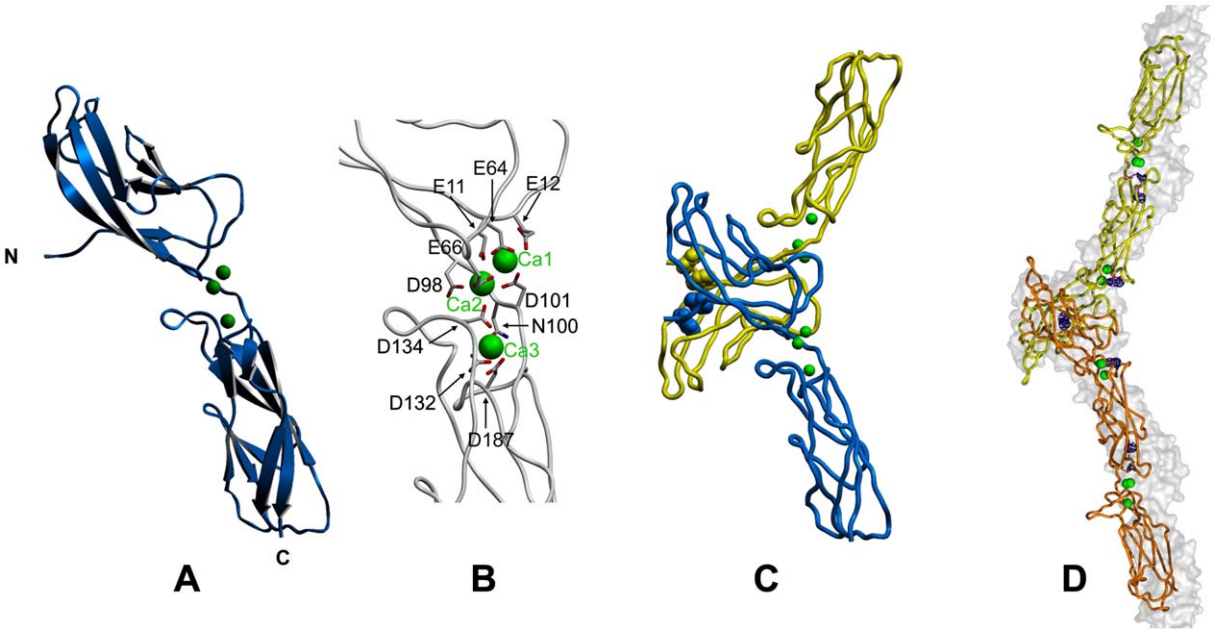

Figure 1. Structure of Multidomain Type II Cadherin Fragments

(A) Ribbon diagram of the cadherin-11 EC1-EC2 structure. Three calcium ions bound at the EC1-EC2 interface are drawn as green spheres.

(B) The interdomain calcium binding site adopts a configuration similar to that observed in type I cadherins. Each of the seven calcium-ligating acidic side chains and the invariant Asn 100 ligand are conserved, and carbonyl oxygens at positions 99, 102, and 141 also donate calcium ligands (not shown), analogous to type I cadherins.

(C) Two crystallographically related protomers join in an interface clearly related to the "strand dimer" interface of type I cadherins, implicated in intercellular adhesion. This interaction is anchored by the insertion of two tryptophan side chains, from the conserved residues Trp2 and Trp4 shown in CPK representation, in the core of the mated protomer. All interactions between mated protomers are within the EC1 domain.

(D) Superposition of the cadherin-8 EC1–EC3 adhesive dimer superimposed on the analogous region from the dimeric five-domain structure of type I C-cadherin, shown as a molecular surface. Anomalous difference electron density, arising from selenomethionine sites, is shown as purple mesh. These sites agree with the modeled methionine positions, providing validation of this low-resolution structure.

proteins diffracted X-rays to resolutions of 2.9 Å, 2.0 Å, and 2.2 Å, respectively. The EC1 domain structure of cadherin-11 reveals a dimer interface that is essentially identical to that seen in the EC1-EC2 construct (see Figure S1 in the Supplemental Data available with this article online), validating the strategy of using EC1 domain crystals for detailed structural analysis of adhesive interfaces.

All three type II cadherin structures reveal similar strand-swapped dimer interfaces, involving the exchange of N-terminal β strands between the partner molecules (Figures 2A–2C). In type II cadherins, the side chains of the critical conserved residues, Trp2 and Trp4 of the swapped A strand, insert into a large pocket in the hydrophobic core of the partner molecule. Type I cadherins (Figure 2D), in contrast, anchor their interfaces by insertion of a single conserved tryptophan, Trp2 (Shapiro et al., 1995a). Sequence conservation of these residues (Figure 3) suggests that this difference in interaction mode—one versus two Trp anchor residues—applies to all type I and type II subfamily members. Of note, many prior binding studies have shown that Trp2 is essential for type I cadherin adhesive function, whereas both Trp2 and Trp4 residues appear essential for adhesive function in VE-cadherin, a divergent member of the type II cadherin family (May et al., 2005).

Adhesive interfaces for the type I and II cadherins have clear similarities in that they form through the swapping of their N-terminal β strands. A number of other features are common to the two interfaces, each involving the swapped β strand. First, the conserved Trp2 and Trp4 side chains in type II cadherins insert into a large hydrophobic pocket lined by residues Leu24, Tyr37, Ala75, Ala77, and Phe92 (Figure 2E). Similarly, the acceptor pocket for the conserved Trp2 side chain in type I cadherins is lined by residues Ile24, Tyr36, 78 (Ala or Ser), Ala80, and 92 (Met or Ile) (Figure 2D). The conserved interaction of Trp2 and Ala80 in type I cadherins is maintained in type II cadherins through the analogous interaction of Trp2 and Ala77. Second, the N terminus in type II cadherins forms a salt bridge with residue Glu87, analogous to the salt bridge formed between the N terminus and Glu89 of type I cadherins. Third, a number of hydrogen bonds are common to both interfaces. These include a conserved hydrogen bond between the ring ε1 nitrogen of Trp2 and the backbone carbonyl of Pro88 in type II cadherins, which is analogous to that between Trp2 and Pro90 in type I cadherins. In

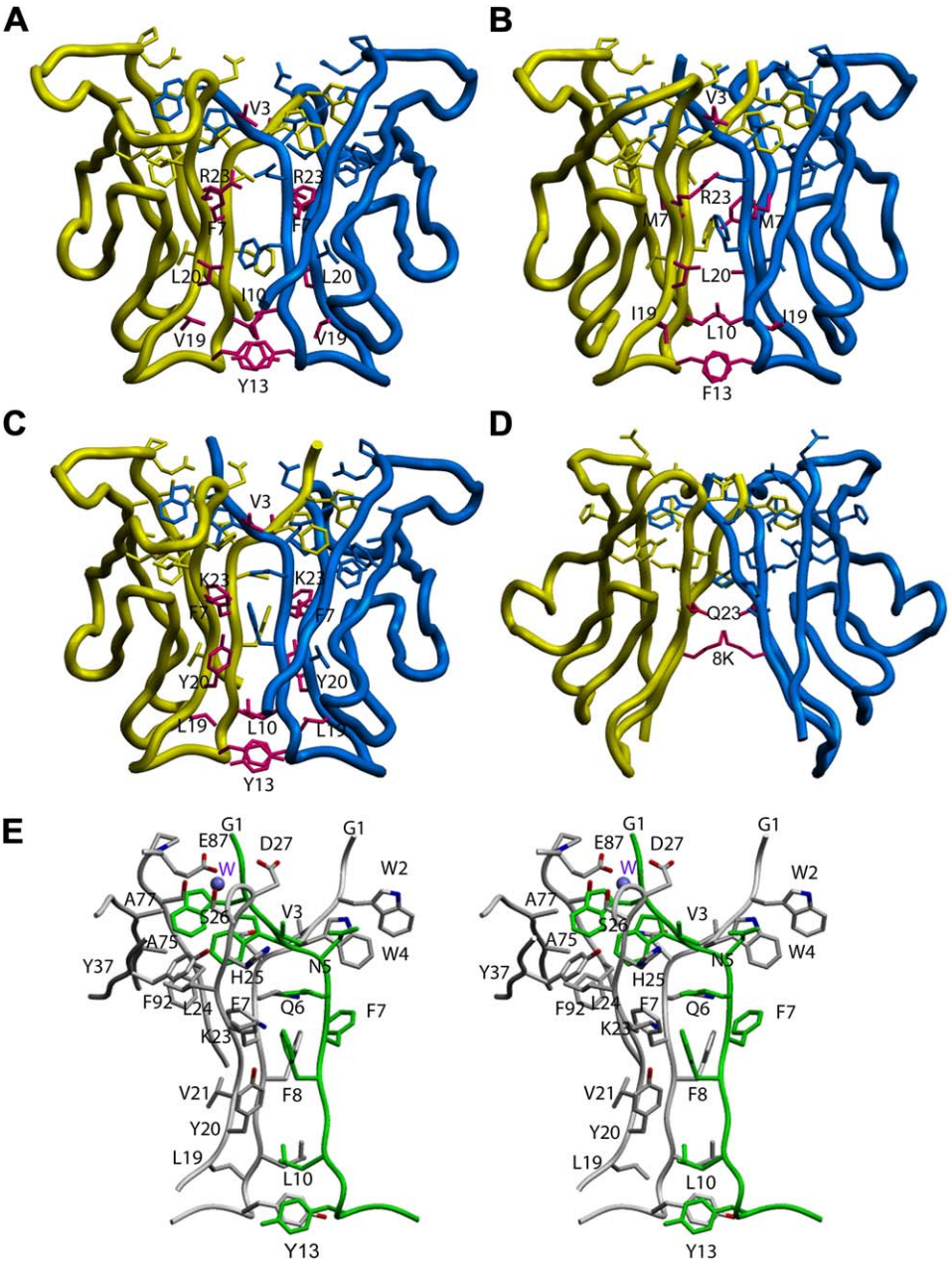

Figure 2. Details of Individual Type II Cadherin Adhesive Interfaces

The 2-fold axis of each interface is oriented vertically: (A) cadherin-11, (B) cadherin-8, and (C) MN-cadherin. Interfacial residues that are conserved among type II cadherins are shown in the same color as the backbone worm (blue or yellow), whereas residues that vary in different type II cadherins and thus may provide binding specificity are shown in magenta. For comparison, the adhesive dimer from the type I family member C-cadherin is shown in (D). A stereo diagram of the adhesive interface from MN-cadherin is shown in (E), with noninteracting regions removed for clarity. A water molecule, labeled W, conserved in type II interface structures, mediates hydrogen bonding interactions between the ring nitrogen of W4 and the side chain hydroxyl group from Ser 90.

addition, a hydrogen bond is formed between the backbone amide of Val3 and the backbone carbonyl of His25, a feature also seen in type I cadherins.

Despite these similarities, there are striking differences between type I and type II adhesive interfaces. The buried accessible surface area in type II cadherins is ~2700–3300 Å^2 (~1350–1650 Å^2 per protomer), whereas type I interfaces are smaller, typically burying ~1600–1800 Å^2. The additional interfacial area in type II cadherins maps to an extended region of nonpolar contacts that contributes to an adhesive interface that runs the entire length of the cadherin EC1 domain. In MN-cadherin, this

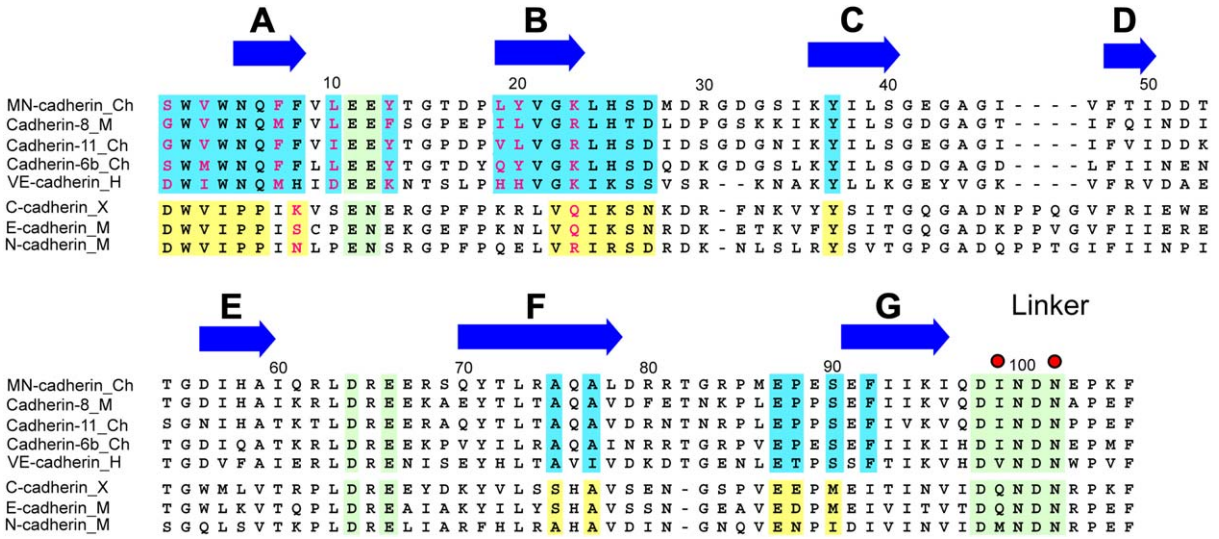

Figure 3. Multiple Sequence Alignment of Type II and Type I Cadherin EC1 Ectodomains

Aligned sequences are shown for representative type II cadherins (MN-cadherin, cadherin-8, cadherin-11, cadherin-6b, and VE-cadherin) and type I cadherins (C-, E-, and N-cadherins) from human (H), mouse (M), chicken (Ch), and *X. laevis* (X). Adhesive interface residues are shaded yellow for type I cadherins and blue for type II. Residues potentially involved in specificity are shown in red. Calcium binding residues are shaded green, with red dots in the linker region indicating residues that coordinate calcium through the backbone carbonyl. Secondary-structure elements for MN-cadherin are indicated above the alignment. VE-cadherin, a divergent type II cadherin, has two conserved Trp residues in the A strand but does not contain all sequence elements characteristic of other type II cadherins.

extended region of hydrophobic interaction contributes ~400 Å^2 of buried surface area and involves the side chains of Phe8, Leu10, Tyr13, Leu19, and Tyr20 (Figure 2E). Phe8 occupies a pocket formed partially by Gly22 and Tyr20 in the partner protomer, and the Phe8 ring stacks directly over the glycine α-carbon. Ile10 fills a pocket formed by Tyr13 and Leu19. Interactions similar to these have not been observed in type I cadherin structures (Figure 2D).

The interdomain angles for the adhesive dimer pairs of cadherin-11, cadherin-8, and MN-cadherin are quite similar—81°, 82°, and 87°, respectively, whereas type I cadherin structures have more highly variable interdomain angles, ranging from 54° to 88° (Figure S2). The smaller range of interdomain orientations observed for type II dimers is probably due to structural constraints imposed by the extended hydrophobic interface. Indeed, as is evident from the sequence alignments (Figure 3) and solvent accessibility surfaces (Figure 4), type II adhesive interfaces extend over the entire length of the EC1 domain, whereas type I cadherin interfaces involve only the upper (N-terminal) half of this domain (Figure 3 and Figure 4). In addition, in molecular surface representations of electrostatic potential, the extended interface region of type II cadherins comprises a single large nonpolar patch (Figure 4A, lower panels), whereas this region of type I cadherins is more polar (Figure 4B, lower panels) and is not involved in interface formation. The adhesive interfaces of the type II cadherin structures presented here reveal a remarkable degree of similarity (Figures 2A–2C). There are no insertions or deletions in the type II cadherin EC1 domains, and, based on structural alignments of Cα atoms, rmsds for any pair of these structures is less than 0.6 Å. Moreover, each interface involves contacts among an identical set of residues: 1–8, 10, 13, 19–27, 75, 77, 87, 90, and 92, each of which is conserved in character in all type II cadherin sequences (Figure 3).

Segregation of Cells Expressing Type I and Type II In Vitro Depends on the EC1 Domain

We examined whether the divergence in EC1 domain structures of type II and type I cadherins is reflected in differences in the adhesive properties of cells expressing these two classes of cadherins in vitro. In these assays, we focused on the adhesive properties of two type II cadherins, MN-cadherin and cadherin-6b, since these two proteins exert different activities in an in vivo assay of neuronal cell sorting (Price et al., 2002). We have not determined the crystallographic structure of cadherin-6b, but sequence alignment indicates that its EC1 domain conforms to the structural features evident in the EC1 domains of MN-cadherin, cadherin-8, and cadherin-11 (74% identity to the EC1 domain of MN-cadherin, 59% to the EC1 domain of cadherin-8, and 61% to the EC1 domain of cadherin-11) (Figure 3).

We produced Chinese hamster ovary (CHO) cell lines that constitutively expressed MN-cadherin; cadherin-6b; and two type I cadherins, N-cadherin and E-cadherin, at similar cell-surface levels (see Experimental Procedures). The adhesive properties of cells expressing each individual cadherin and pair-wise combinations of type II and type I cadherins were then tested using a standard

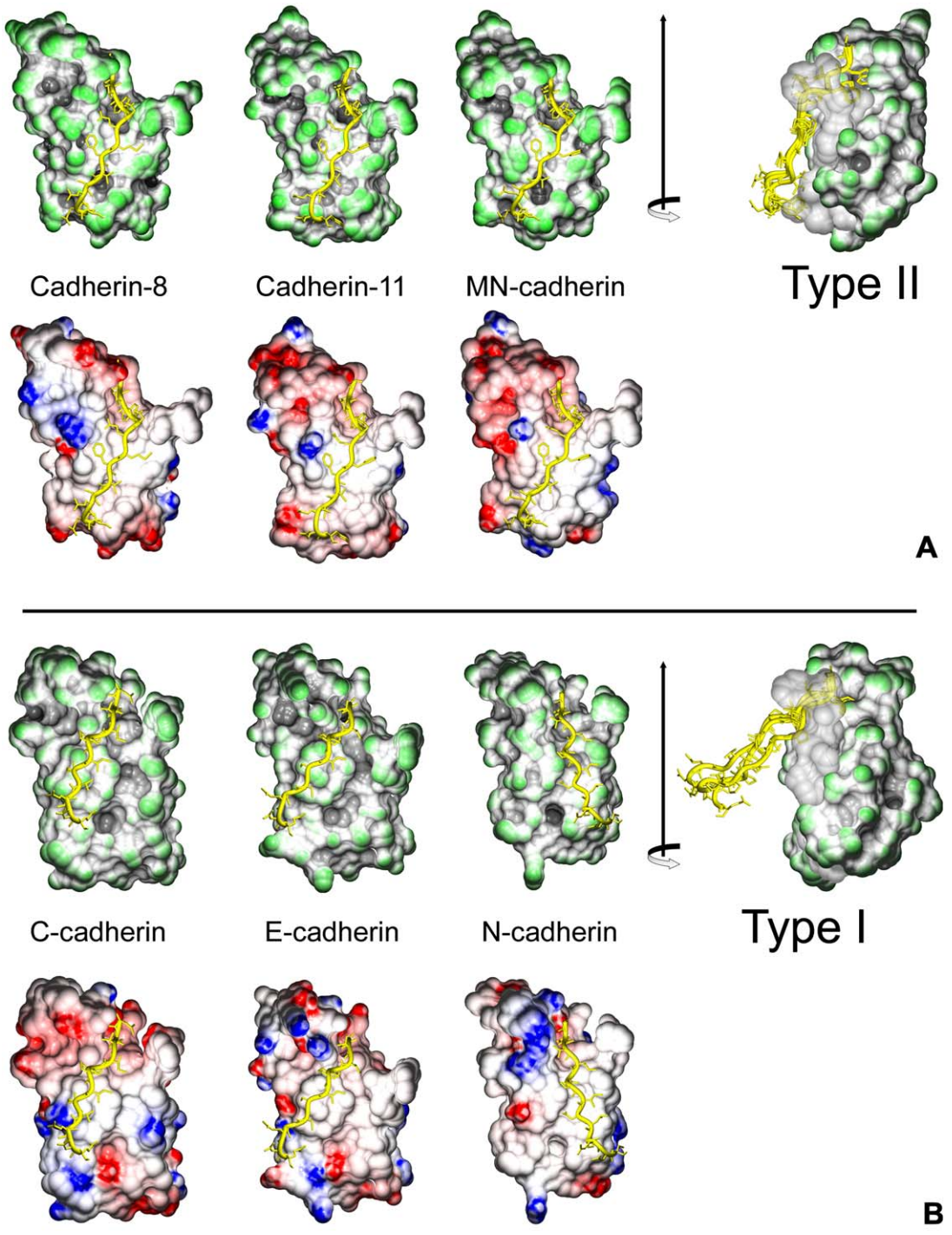

Figure 4. Comparison of Binding Surfaces for Type II Cadherins and Type I Cadherins

Both convexity/concavity surfaces (green and white) and charge potential surfaces, from −10 kT (red) to +10 kT (blue), are shown mapped onto EC1 protomers; the corresponding A strands from the dimer partner are shown in yellow. Note the similarity in shape of type II cadherins and the large nonpolar region that define the path of the A strands in type II cadherins (A). The right panel shows the molecular surface from MN-cadherin, with A strands from cadherin-8, MN-cadherin, and cadherin-11 superposed. Type I interfaces (B) lack the nonpolar extended interface region of type II cadherins, and their A strands can thus adopt structures that are far more variable. This can be seen in the right panel, which shows a molecular surface of C-cadherin EC1 with superposed A strands from C-, E-, and N-cadherins. Residues 1–13 of the A strand were used for each figure.

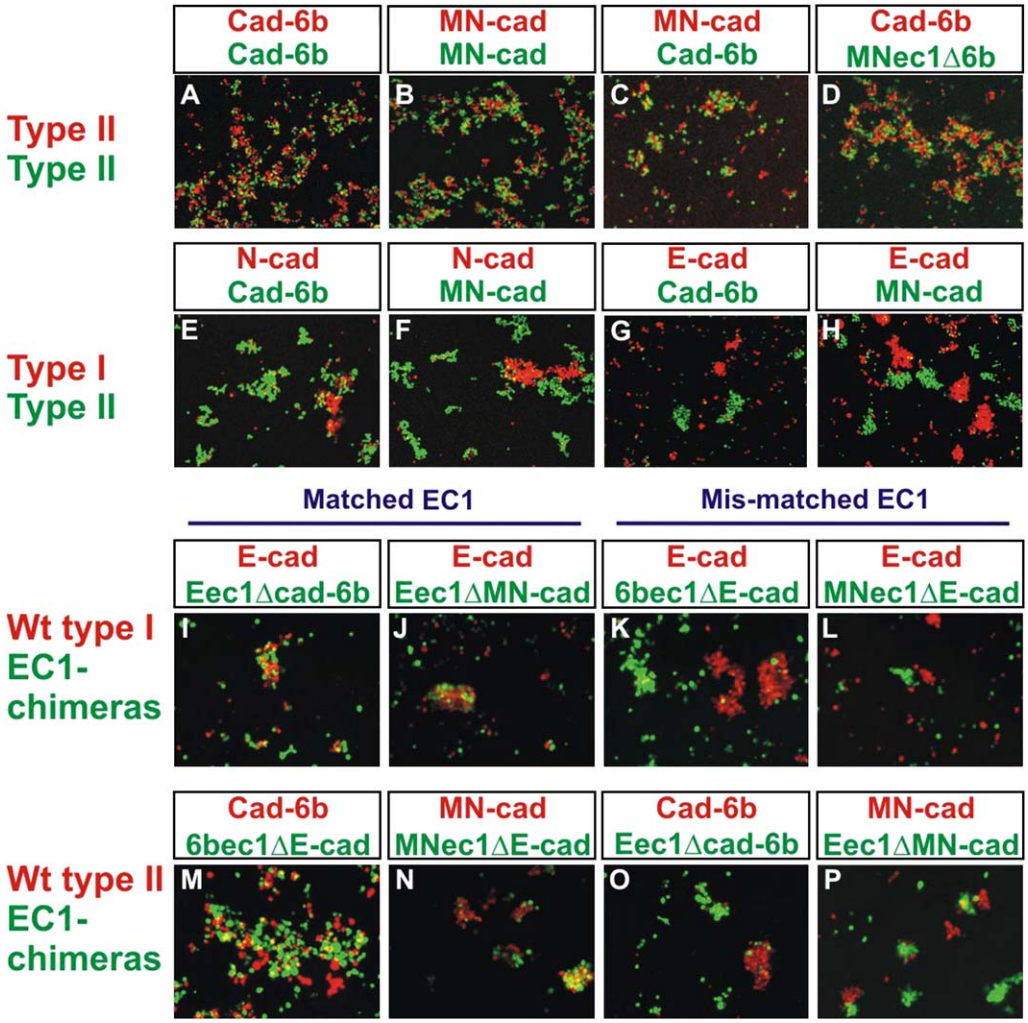

Figure 5. Aggregation Cadherin and Cadherin-Chimera-Expressing CHO Cells

(A–D) Type II/II cadherin short-term coaggregation assays (similar mixed cell aggregates are found in long-term assays).

(E–H) Type I/II long-term coaggregation assays. Type I expressors and type II expressors form segregated cell aggregates.

(I–P) Coaggregation experiments with cadherin chimeras show that the first extracellular domain is necessary to confer subtype specificity of aggregation of type I and type II cadherins.

(I–L) E-cadherin expressors forms mixed aggregates with cells expressing chimeras that have an E-cadherin EC1 domain but segregate from cells expressing chimeras with EC1 domains from type II cadherins.

(M–P) Conversely, type II cadherin-6b and MN-cadherin form mixed aggregates with chimeras containing a type II EC1 domain but segregate from chimeras with an E-cadherin EC1 domain.

aggregation assay (Tamura et al., 1998). Cells expressing each type I and type II cadherin formed large aggregates in the presence of extracellular calcium, but no aggregation was observed when cells were maintained in the presence of the calcium chelator EGTA (data not shown). Calcium dependence is a hallmark of cadherin-mediated cell adhesion (Takeichi et al., 1981), indicating that the observed cellular aggregation properties of both type II and type I cadherins arise from their calcium-dependent homophilic adhesive interactions.

We next tested the ability of cells expressing type II cadherins to interact with cells expressing type I cadherins. Coaggregation assays were performed with cells expressing MN-cadherin or cadherin-6b mixed with cells expressing E-cadherin or N-cadherin. We found that the aggregates formed by cells expressing cadherin-6b segregated from aggregates of cells expressing N-cadherin or E-cadherin (Figures 5E and 5G). Similar findings were obtained with mixtures of cells expressing MN-cadherin and N-cadherin or E-cadherin (Figures 5F and 5H). Assays of E-cadherin- and N-cadherin-expressing cells revealed a level of coaggregation similar to that found between cells expressing type I and type II cadherins (data not shown). These findings confirm and extend studies

demonstrating the segregation of cells expressing other type II and type I cadherins (Shimoyama et al., 1999; Nakagawa and Takeichi, 1995).

To investigate the contribution of EC1 domains to the specificity of cadherin adhesive interactions, we produced chimeric expression constructs in which the EC1 domains were shuffled between cadherins. Four domain-shuffled constructs were produced: one in which MN-cadherin EC1 was fused to the EC2 through the C-terminal region of cadherin-6b (MNEC1Δ6b), a complementary chimeric construct in which the EC1 domain of cadherin-6b was fused to the EC2 through C-terminal region of MN-cadherin (6bEC1ΔMN), and two chimeras in which the type I EC1 domain from E-cadherin was grafted to EC2 through C-terminal regions from the type II cadherins (Eec1Δcadherin-6b and Eec1ΔMN-cadherin) (see Figure 6A). CHO cells expressing each EC1 domain-shuffled chimera showed calcium-dependent self-aggregation. In mixed cell-aggregation assays, the identity of the EC1 domain was found to determine the specificity of cell segregation. Thus, Eec1Δcadherin-6b and Eec1ΔMN-cadherin formed mixed aggregates with E-cadherin cells (Figures 5I and 5J) but segregated from cadherin-6b and MN-cadherin cells, respectively (Figures 5O and 5P). Similarly, 6bec1ΔE-cadherin and MNec1ΔE-cadherin segregated from E-cadherin cells (Figures 5K and 5L) but formed mixed aggregates with cadherin-6b and MN-cadherin cells, respectively (Figures 5M and 5N). These findings support the view that the EC1 domain is a major determinant of the specificity of interaction between type I and type II cadherins.

The EC1 Domain Is a Primary Determinant of Recognition Specificity between Type II Cadherins In Vivo

We next turned to the issue of whether interactions between type II cadherins are dependent on structural features resident within the EC1 domains of these proteins. Evidence that type II cadherin subfamily members exhibit recognition specificity has come from an analysis of the distinct activities of MN-cadherin and cadherin-6b in the regulation of motor neuron sorting in the chick spinal cord in vivo (Price et al., 2002).

Coaggregation assays of cells expressing either cadherin-6b or MN-cadherin failed to reveal adhesive specificity, despite the use of a wide variety of cell-aggregation conditions (see Experimental Procedures). The resulting cell aggregates were composed of cells expressing each cadherin (Figure 5C), and the extent of coaggregation was similar to that obtained with aggregation of each cadherin cell population independently (Figures 5A and 5B). Moreover, cells expressing MNEC1Δ6b or 6bEC1ΔMN exhibited Ca^{2+}-dependent aggregation behavior in both self-aggregation (data not shown) and coaggregation assays (Figure 5D and data not shown). Similar mixed aggregates were obtained between 6bEC1ΔE and MN-cadherin cells (data not shown). These results show that cadherin chimeras are functional in that they mediate cell aggregation like the parent proteins. However, the mixed aggregation behavior of cells expressing different type II cadherins suggests that this in vitro assay is not appropriate for revealing adhesive specificity among type II cadherins. We therefore turned to an in vivo assay of motor neuron sorting to explore whether the EC1 domain interfaces of type II cadherins encode their functional specificity.

In the lumbar spinal cord of chick embryos, individual motor pools can be characterized by their distinct profile of expression of type II cadherins (Price et al., 2002). Furthermore, in vivo misexpression studies have shown that the normal developmental segregation of adductor (A), femorotibialis (eF), and hip retractor (HR) motor neurons depends on the selectivity of MN-cadherin expression but is uninfluenced by their cadherin-6b profile. Thus, ectopic expression of MN-cadherin in HR or eF motor neurons prevents their segregation from A motor neurons (Figures 6E–6G; Price et al., 2002), whereas motor pool segregation is not impaired by elevated cadherin-6b expression (Price et al., 2002; data not shown). This analysis of motor neuron pool sorting provides an in vivo context in which MN-cadherin and cadherin-6b have distinguishable activities and thus permits an assessment of the consequences of interchanging the EC1 domains of MN-cadherin and cadherin-6b on cell mixing.

We examined the activity of a chimeric type II cadherin in which the EC1 domain of cadherin-6b replaces the corresponding EC1 domain of MN-cadherin (6bEC1ΔMN). Ectopic expression of 6bEC1ΔMN did not impair the normal segregation of A from HR or of A from eF motor pools (Figures 6H–6K) as assessed by the diagnostic pool-specific profiles of ETS and LIM homeodomain transcription factors (A: $Isl1^{+}/Er81^{+}$; eF: $Isl1^{-}/Er81^{+}$; HR: $Isl1^{+}/Er81^{-}$; see figure legend). Thus, substitution of the EC1 domain of MN-cadherin by that of cadherin-6b abolishes the wild-type activity of MN-cadherin. More intriguingly, the 6bEC1ΔMN chimera fails to mimic the activity of MN-cadherin in motor neuron pool sorting in vivo, despite its ability to interact with MN-cadherin in an in vitro assay of cell aggregation.

Conversely, we examined whether a chimeric type II cadherin in which the EC1 domain of MN-cadherin replaces the corresponding EC1 domain of cadherin-6b (MNEC1Δ6b) is able to impair motor neuron pool sorting in manner reflective of the activity of wild-type MN-cadherin. Expression of MNEC1Δ6b resulted in a significant impairment in the normal segregation of A and HR motor neurons as assessed by the mixing of $Isl1^{+}/Er81^{+}$ and $Isl1^{+}/Er81^{-}$ motor neurons (Figures 6M and 6O). Both electroporated as well as nonelectroporated HR motor neurons were significantly perturbed in their normal segregation from A motor neurons, as after MN-cadherin misexpression (Figure 6O; Figure S4D; Price et al., 2002). Thus, insertion of the first extracellular domain of MN-cadherin is sufficient to confer MN-cadherin-like activity to an otherwise inert cadherin-6b protein. Expression of MNEC1Δ6b also resulted in a significant impairment in the normal segregation of A and eF motor neurons as assessed by the

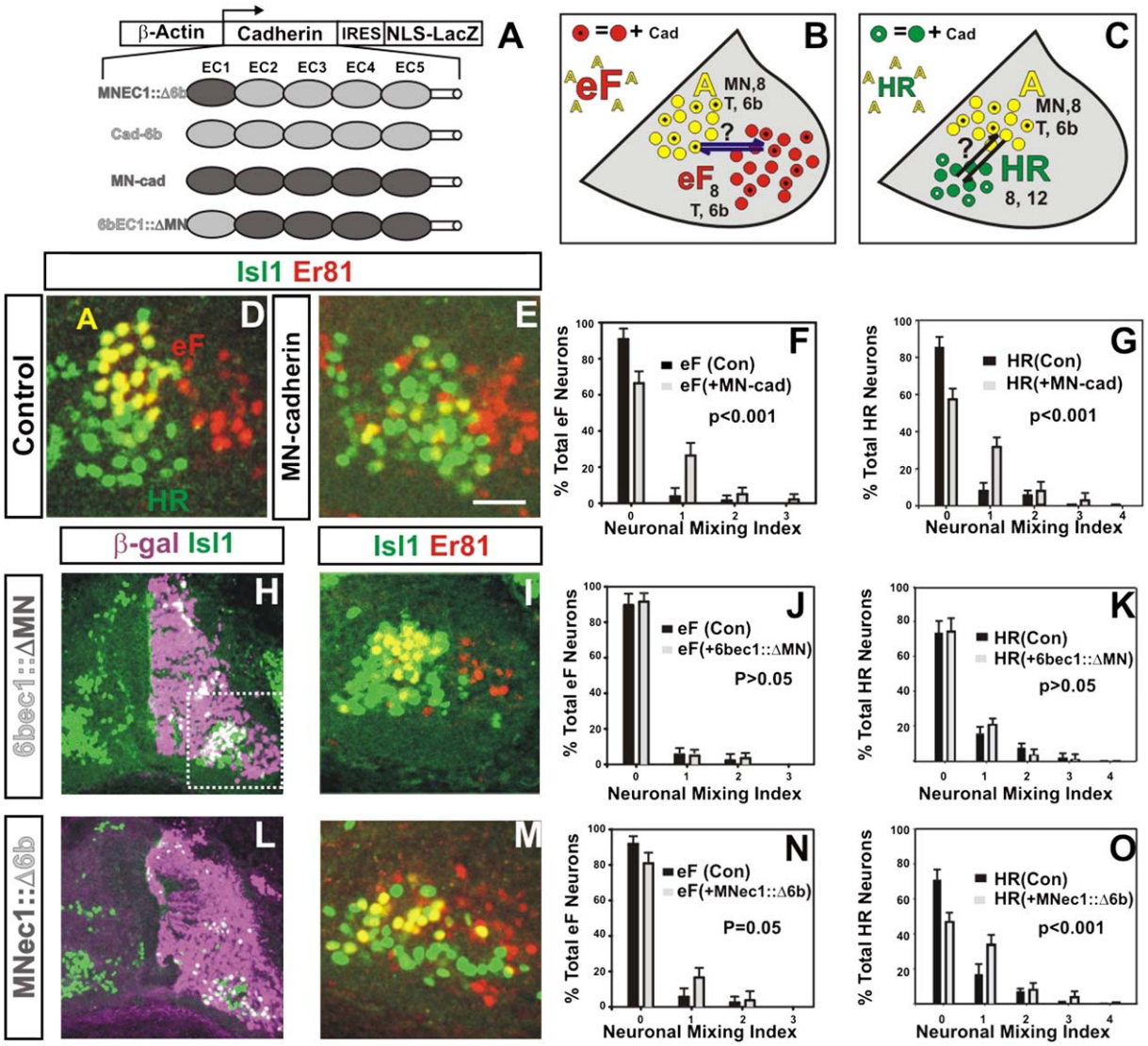

Figure 6. Motor Neuron Pool Sorting Elicited by Misexpression of Chimeric Type II Cadherins

(A) Schematic of chimeric constructs.

(B and C) Positioning of adductor (A, yellow), femorotibialis (eF, red), and hip retractor (HR, green) motor pools and their cadherin expression profiles.

(D–G) MN-cadherin misexpression causes a desegregation of A and eF and of A and HR motor pools. (Reprinted from *Cell* 109, Price et al., Regulation of motor neuron pool sorting by differential expression of type II cadherins, pp. 205–216, copyright 2002, with permission from Elsevier.)

(F and G) Quantitation of motor neuron pool mixing following MN-cadherin misexpression.

(H–K) Misexpression of 6bEC1ΔMN-cadherin appears to have no effect on A-eF and A-HR motor pool segregation.

(J) Quantitation of A-eF motor pool segregation following 6bEC1ΔMN-cadherin misexpression. χ^2 analysis $p > 0.05$, total of 365 eF neurons from three embryos, electroporation efficiency of 64%.

(K) Quantitation of A-HR motor pool segregation following 6bEC1ΔMN-cadherin misexpression. χ^2 analysis $p > 0.05$, total of 918 HR neurons from three embryos, electroporation efficiency of 61%.

(L–O) MNEC1Δ6b misexpression results in a significant perturbation of A-HR and A-eF motor pool segregation.

(N) eF neurons are perturbed in their segregation from A neurons, albeit at a level reduced from that seen with MN-cadherin misexpression (Price et al., 2002). χ^2 analysis $p = 0.05$, total of 422 eF neurons from four embryos, electroporation efficiency of 60%.

(O) HR neurons are significantly perturbed in their segregation from A neurons following MN-cadherin misexpression. χ^2 analysis $p < 0.001$, total of 1099 HR neurons from four embryos, electroporation efficiency of 56%. Scale bar is 50 μm in (D), (E), (I), and (M) and 150 μm in (H) and (L). Error bars in (F), (G), (J), (K), (N), and (O) show mean ± standard deviation.

intermixing of Isl1$^+$/Er81$^+$ and Isl1$^-$/Er81$^+$ motor neurons (Figures 6M and 6N). The impairment in segregation of eF and A motor neurons was restricted to electroporated neurons, a finding similar to that obtained with native MN-cadherin. However, the extent of A and eF mixing elicited by MNEC1Δ6b expression was less pronounced

than that obtained after expression of wild-type MN-cadherin (Figures 6E and 6O; Price et al., 2002). Nevertheless, when taken together with the pronounced intermixing of A and HR neurons, these findings provide evidence that the EC1 domains of type II cadherins are a major determinant of recognition specificity in vivo.

DISCUSSION

The interaction specificity of classical cadherins is thought to underlie many aspects of tissue assembly and organization. The structural basis of cadherin recognition has remained contentious, however, with different experimental approaches and findings lending support for markedly divergent views on the precise protein subdomains responsible for cadherin binding and on the extent of specificity in the interactions of different cadherins. In this study, we report the crystal structures of extracellular domains from three type II cadherins, revealing that, although there are shared aspects of type I and type II cadherin structure, notably the reliance on the EC1 domain for adhesive interaction, there are also significant differences in the details of their interaction. The comparative information on type II and type I cadherin structures that emerges from this analysis provides a basis for interpretation of the binding and recognition specificities of the classical cadherins.

The EC1 Domain Interface Mediates Adhesion in Type II Cadherins

The molecular identity of the cadherin adhesive interface has been a matter of controversy. Crystallographic studies of type I cadherins have indicated that adhesive contacts involve exclusively the EC1 domain, though other biologically relevant conformations involving interactions in other regions cannot be ruled out (Boggon et al., 2002). Electron micrographic studies of cadherin-based desmosomal junctions have similarly implicated extreme amino-terminal binding interactions (He et al., 2003) and are therefore consistent with crystallographic evidence. Biochemical evidence also supports a pivotal role for the EC1 domain: Cell-aggregation experiments with swapped EC1 domains in type I cadherin chimeras have demonstrated that cell-mixing behavior is determined by the identity of this domain (Nose et al., 1990; Shan et al., 1999, 2000), and crosslinking studies are also consistent with this view (Harrison et al., 2005; Troyanovsky et al., 2003). In contrast, the findings of studies of cadherin interaction based on atomic force microscopic (AFM) and force spectroscopic analyses have revealed a number of characteristic forces between interacting cadherins that are difficult to interpret solely in terms of adhesive interactions located on the EC1 domain (Perret et al., 2004; Zhu et al., 2003). These observations have led to the proposal that cadherin binding involves the interdigitation of multiple EC domains and thus an interaction over the entire ectodomain (Chappuis-Flament et al., 2001; Sivasankar et al., 1999). Further, a recent deletion mutagenesis study of N-cadherin has suggested a requirement for two domains (EC1-EC2) for adhesion of transfected cells to N-cadherin-coated slides (Shan et al., 2004).

One clear finding of the present structural analysis is that type II cadherins exploit a dimerization mode that depends on the EC1 domain, and, thus, the topology of their interactions exhibits many features in common with that of type I cadherins. The critical role of the EC1 domain in binding interactions that now emerges from multiple crystallographic studies of members of both classical cadherin subfamilies adds support to the view that the biologically relevant adhesive interface in classical cadherins is restricted to the EC1 domain. Together, our findings and the many others cited above favor a unified structural picture of the nature of cadherin-mediated cell adhesion, one that involves, largely or exclusively, interactions between the EC1 domains of interacting protein partners. Our studies cannot exclude that some biologically relevant cadherin conformations involve interactions between other EC domains. But, in the light of our findings, it may be necessary to seek alternate explanations for AFM and force spectroscopic studies that have revealed a diverse hierarchy of rupture strengths for bonds between cadherin extracellular regions (Perret et al., 2004; Zhu et al., 2003). Although these studies have been interpreted as evidence for cadherin interactions that involve domains other than EC1, the structural basis of these postulated alternative binding modes is not clear.

A Strand-Exchange Mechanism within the EC1 Domain Interface Mediates Adhesion in Type II Cadherins

How are adhesive interactions achieved between the EC1 domains of interacting type II cadherins? Our findings provide evidence that, in type II cadherins, the amino-terminal A strand is swapped between EC1 domains presented from juxtaposed cell surfaces so as to form symmetrical dimers. Although monomer structures have not yet been determined for any type II cadherin, these proteins are monomeric at low concentrations (C.C. and L.S., unpublished data), suggesting that they adopt a "closed" monomer form in which the swapped strand is inserted into its own protomer body in a manner similar to that observed for the closed monomer form of E-cadherin (Pertz et al., 1999).

Nevertheless, there appear to be marked differences in the details of the strand-swap mechanism in type II and type I cadherins. In type II cadherins, the swapped strand includes two key tryptophan residues, whereas in type I cadherins, the swapped domain contains a single interactive tryptophan (Boggon et al., 2002; Haussinger et al., 2004; Shapiro et al., 1995a). Conversely, the strand acceptor pocket within the EC1 domain of type II cadherins is, by necessity, far larger than that for type I cadherins. These structural inferences are supported by biochemical data indicating that mutation of the Trp2 residue in type I cadherins (Shan et al., 1999; Tamura et al., 1998) and either Trp2 or Trp4 in type II cadherins (May et al., 2005) abolishes cell-cell adhesion. The apparent requirement

for the EC2 domain in cadherin binding under certain experimental conditions (Shan et al., 2004) is likely to reflect the fact that the strand-exchange reaction is catalyzed by calcium binding between the EC1 and EC2 domains (Haussinger et al., 2004). Moreover, the buried accessible surface area in type II cadherins is almost twice that for type I cadherins. This additional interfacial area in type II cadherins maps to an extended region of nonpolar contacts, establishing an adhesive interface that runs the entire length of the cadherin EC1 domain. Thus, adhesive interactions between the EC1 domains of type II cadherins differ significantly from those of type I cadherins.

Structural Basis of Classical Cadherin Adhesive Specificities

Comparison of the topological features of the EC1 domains of type II and type I cadherins predicts that they will fail to form effective adhesive interactions. Two key structural features are likely to underlie the orthogonal binding specificities of type I and type II cadherins. First, the conservation of two tryptophan anchor residues in the swapped A strand of type II cadherins is incompatible with the acceptor pocket of type I cadherins, which is appropriately sized to bind only a single tryptophan side chain. Second, the extended region of hydrophobic interaction common to type II adhesive interfaces is incompatible with the hydrophilic surfaces of corresponding regions in type I cadherins (Figure 4). These molecular differences appear therefore to make type I and type II cadherins incompatible binding partners. Consistent with these observations, our domain-shuffling experiments reveal that the EC1 domain defines subfamily-restricted adhesive specificity in molecular chimeras of type I and type II cadherins. These findings provide a basis for interpretation of other functional studies that reveal a lack of cross-interaction between type I and type II cadherins (this work; Shimoyama et al., 2000; Duguay et al., 2003; Foty and Steinberg, 2005; Niessen and Gumbiner, 2002; Shan et al., 2000) and between different type II family members (Shimoyama et al., 1999, 2000).

The dimeric adhesive interfaces of the EC1 domains of the three type II cadherin structures presented here reveal a remarkable degree of similarity, whereas a much greater degree of diversity is evident in equivalent type I cadherin domains (Boggon et al., 2002; Haussinger et al., 2004; Shapiro et al., 1995a). These observations raise the issue of whether—and, if so, how—individual type II cadherins acquire specificity in their recognition of other type II family members. Our findings and those of others (Shimoyama et al., 1999, 2000) show that different type II cadherins exhibit extensive heterotypic coaggregation when assessed by in vitro cell-aggregation assays. In contrast, equivalent in vitro conditions permit selective adhesive interactions between type I cadherins (Nose et al., 1990; Shan et al., 1999, 2000). Thus, the structural conservation of type II cadherin EC1 domains appears to be reflected in a greater propensity for heterophilic binding when compared with type I cadherins.

Nevertheless, in vivo assays of motor neuron sorting in the developing spinal cord have provided evidence that type II cadherins, notably MN-cadherin and cadherin-6b, have distinct influences on motor neuron sorting (Price et al., 2002), implying differences in their adhesive or recognition properties. This in vivo assay has permitted a test of the structural prediction that recognition specificity within type II cadherins maps largely or exclusively to the EC1 domain. We find that the EC1 domain is a major interacting interface between cadherin monomers and that the influence of wild-type MN-cadherin on motor neuron sorting can be reproduced in large part by a chimeric protein in which the EC1 domain of MN-cadherin replaces the corresponding domain of cadherin-6b. However, the effect on A and eF motor neuron sorting of MNEC1Δ6b misexpression is attenuated compared to wild-type MN-cadherin. It is possible that the chimeric structure perturbs the adhesive properties of the EC1 domain, diminishing its activity without altering its recognition specificity. For example, since calcium binding between EC1 and EC2 is known to kinetically enhance domain swap binding (Haussinger et al., 2004), perturbations of this region could alter adhesiveness. Nonetheless, our studies emphasize the importance of the EC1 domain for type II cadherin recognition specificity.

What might account for the divergent findings on specificity of interactions between different type II cadherin family members that emerge from in vitro and in vivo assays? One striking difference in the starting conditions of these in vitro and in vivo studies is that multiple type II family members are expressed by each motor neuron (Price et al., 2002; Redies et al., 2003), and this feature is therefore poorly modeled by cells expressing single cadherins in vitro. The native expression of multiple type II cadherins in single cells suggests the potential for their combinatorial function in cell recognition. We (Boggon et al., 2002) and others (He et al., 2003) have reported preliminary structural evidence for *cis* interactions between cadherin molecules presented on the same cell surface, raising the possibility that multicadherin complexes could extract specificity from the identity of each component cadherin. In addition, classical cadherins have been shown to form cell-surface complexes with nectins, a second class of adhesive proteins (Tanaka et al., 2003), raising the possibility that the relevant context for selectivity in type II cadherin recognition involves a heteromeric cadherin-nectin complex.

It is also possible that the forces exerted on neurons and other cells in vivo and the time course of cellular segregation during development are radically different from those operating in simplified in vitro assay systems. Cadherin specificity may thus depend critically on the precise conditions of such forces. Insights into the subtleties of classical cadherin recognition specificity have also emerged from recent theoretical studies that have suggested how domain swapping enables small differences in cadherin molecular affinity to yield adhesive selectivity at the cellular level (Chen et al., 2005). A more quantitative understanding of cadherin-based cell adhesion requires that surface

Table 1. Statistics from the Crystallographic Analysis

Protein	MN EC1	Cad8 EC1	Cad11 EC1	Cad11 EC1-2	Cad8 EC1–3
Space group	$P2_1$	$P2_1$	$P3_221$	$P6_222$	$P4_122$
Unit cell	a = 32.3, b = 76.1, c = 37.1, β = 96.0°	a = 46.2, b = 39.9, c = 66.5, β = 110.7°	a = 76.94, c = 102.3	a = 203.3, b = 42.8	a = b = 75.8, c = 233.7
Molecules per asymmetric unit	2	2	2	1	1
Resolution limit (Å)	2.2	2.0	2.9	3.2	4.5
Unique reflections	9,186	15,327	8,099	8,610	4,479
Redundancy	17.6	3.7	5.2	16.5	13.2
Completeness, high-resolution shell (%)	99.7 (97.9)	99.1 (93.4)	99.9 (100)	99.9 (100)	100.0 (100.0)
Average I/σ (I)	17.1 (6.4)	10.7 (4.5)	17.4 (4.5)	33.3 (11.6)	20.9 (7.5)
R_{merge} (%)	9.4 (27.0)	10.0 (25.2)	9.6 (42.1)	8.3 (32.8)	14.8 (48.1)
Refinement					
R_{work} (%)	19.1	24.1	22.3	21.7	27.2
R_{free} (%)	24.4	28.8	26.4	24.5	34.9
Rmsd bonds (Å)	0.005	0.014	0.013	0.010	0.013
Rmsd angles (°)	1.307	1.639	1.614	1.372	1.790
Protein atoms	1,534	1,546	1,542	1,616	2,484
Water molecules	201	108	0	18	0
Average B ($Å^2$) (protein atoms)	20.46	26.7	34.7	74.9	166.4
Average B ($Å^2$) (water molecules)	31.8	33.3		62.9	
Ramachandran Plot Regions					
Most favored (%)	89.2	85.8	87.8	83.1	68.3
Additionally allowed (%)	10.8	11.7	10.4	15.8	21.9
Generously allowed (%)	0.0	1.9	1.2	1.1	7.2
Disallowed (%)	0.0	0.6	0.0	0.0	2.5
MN-EC1 MAD Experiment	Peak	Edge			
Wavelength (Å)	0.9791	0.9794			
Resolution limit (Å)	2.6	2.6			
Unique reflections	5,612	5,556			
Redundancy	12	13.1			
Completeness (%)	99.6 (99.7)	99.7 (99.5)			
Average I/σ (I)	18.0 (9.1)	17.7 (7.0)			
R_{merge} (%)	7.3 (15.3)	7.9 (20.7)			
Phasing Power					
Acentrics (Bijvoet)	2.07 (1.41)	1.79 (1.11)			
Acentrics (dispersive)	2.14 (1.52)				
Centrics (dispersive)	1.53 (0.95)				

cadherin concentration, cadherin affinities, and intercellular forces be measured precisely under relevant physiological conditions.

The domain-swapping strategy evident in classical cadherin interactions may also extend to other classes of proteins involved in homophilic cell adhesion. Domain swapping is likely to drive adhesive interactions between desmosomal cadherins, in which residues critical for classical cadherin strand swap dimerization are conserved (Patel et al., 2003). A domain swapping mechanism has

also been suggested to account for the homophilic binding of hemolins and L1 proteins, immunoglobulin-like families of adhesion proteins (Su et al., 1998). The underlying rationale of domain swapping may therefore have general relevance to adhesive interactions that direct tissue assembly.

EXPERIMENTAL PROCEDURES

Protein Expression, Purification, and Crystallization

Proteins for structural analysis were expressed in the prokaryotic pSMT3 SUMO/His-tag fusion system and purified by affinity chromatography, tag cleavage, ion exchange, and size exclusion. All EC1 domain constructs encoded residues 1–98; EC1-2 encoded 1–207; EC1–3 encoded 1–322. Crystallization screening was performed in 96-well sparse matrix screens and optimized in 24-well hanging-drop experiments. Details are given in the supplemental section.

Data Collection and Processing

Data from selenomethionine-substituted crystals were collected at the NSLS beamline X9A for MN-cadherin EC1 and at beamline ID-31 of the Advanced Photon Source for cadherin-8 EC1–3. Native data sets were collected at beamline X4A of the National Synchrotron Light Source (cadherin-11 EC1 and cadherin-11 EC12) and at beamline ID-31 of the Advanced Photon Source (cadherin-8 EC1). All data were processed and scaled using the HKL program suite, Denzo, and Scalepack (Otwinowski and Minor, 1997). Data processing statistics are shown in Table 1.

Structure Solution and Refinement

The crystal structure of MN-cadherin EC1 was determined using phases obtained from a two-wavelength MAD experiment performed on a single selenomethionine-substituted crystal, and other structures were determined using this structure as a molecular-replacement search model. Details are given in the Supplemental Data.

Generation of Cadherin Constructs for Eukaryotic Expression

Stable cell lines expressing cadherins and cadherin chimeras were prepared using the pCDNA5 expression vector. For in ovo misexpression, cadherin and chimeric cadherin cDNAs were cloned into a pCAGGS vector containing an internal ribosome entry sequence (IRES) followed by a cDNA encoding a nuclear-localization sequence-tagged β-galactosidase. Details are given in the Supplemental Data.

Aggregation Assays

We used two different aggregation assays in this work, "long-term" and "short-term" assays, as described by Shimoyama et al. (2000), with time courses of 12–24 and 1–2 hr, respectively. Dispersed cell suspensions were obtained by treating confluent CHO cells with enzyme-free cell-dissociation solution (Sigma) at 37°C for 10 min and were resuspended in Dulbecco's Modified Eagle's Media (DMEM) containing 10% fetal calf serum and 70 units of DNase I. 5×10^4 cells per 0.5 ml were added to 24-well ultra-low cluster plates (Corning Costar, Cambridge, MA, USA) and allowed to aggregate at 37°C on a rotary shaker at 70–80 revolutions per minute in a humidified atmosphere of 5% CO_2/95% air. For short-term assays, Hank's balanced salt solution was used for cell resuspension. To attempt to uncover specificity of adhesion of mixed aggregates, we systematically varied several parameters of the aggregation assay. Calcium concentrations were varied between 0.1 mM and 10 mM, the total number of cells per aggregation assay was varied from 5×10^4 to 2.5×10^5, and effects of shear forces were assessed by varying rotation speeds between 30 and 100 rpm. Aggregation time courses from 1 hr to 24 hr were evaluated. See Supplemental Data for details.

Chick-Embryo Preparation

Chick eggs (Spafas, Truslow Farms, and Henry Stewart and Company) were incubated and staged as previously described (Hamburger and Hamilton, 1951). Expression of cDNAs was achieved by in ovo electroporation using an ECM830 electro-squareporator (BTX, Inc.). Pulses were of 50 ms duration and 950 ms pulse interval five times at 30V. Embryos were electroporated at HH stages 15–18 and analyzed at HH stages 28–30. Analysis of neuronal mixing was performed as described previously (Price et al., 2002). Antibodies used in this study were: Guinea pig anti-Isl1(2) (1/20000), Goat anti-β-galactosidase (1/1000), mouse anti-Er81 (1/50). Immunocytochemistry was performed essentially as described (Price et al., 2002).

Supplemental Data

Supplemental Data include Supplemental Experimental Procedures, Supplemental References, and four figures and can be found with this article online at http://www.cell.com/cgi/content/full/124/6/1255/DC1/.

ACKNOWLEDGMENTS

This work was supported in part by NIH grants GM-062270 (L.S.) and GM-30518 (B.H.); Wellcome Trust Grant 072914 (S.R.P.); and the RPB foundation (L.S.). T.M.J. and B.H. are investigators of the Howard Hughes Medical Institute. T.M.J. was supported by a grant from NCI. We are grateful for use of beamlines X4 and X29 at the National Synchrotron Light Source at Brookhaven National Laboratory. Use of the SGX-CAT beamline facilities (ID-31) at the Advanced Photon Source was provided by Structural GenomiX, Inc., who constructed and operates the facility. We thank Prof. Richard Axel for helpful discussions.

Received: May 4, 2005
Revised: December 1, 2005
Accepted: December 29, 2005
Published: March 23, 2006

REFERENCES

Bekirov, I.H., Needleman, L.A., Zhang, W., and Benson, D.L. (2002). Identification and localization of multiple classic cadherins in developing rat limbic system. Neuroscience *115*, 213–227.

Boggon, T.J., Murray, J., Chappuis-Flament, S., Wong, E., Gumbiner, B.M., and Shapiro, L. (2002). C-cadherin ectodomain structure and implications for cell adhesion mechanisms. Science *296*, 1308–1313.

Chappuis-Flament, S., Wong, E., Hicks, L.D., Kay, C.M., and Gumbiner, B.M. (2001). Multiple cadherin extracellular repeats mediate homophilic binding and adhesion. J. Cell Biol. *154*, 231–243.

Chen, C.P., Posy, S., Ben-Shaul, A., Shapiro, L., and Honig, B. (2005). Dynamic domain swapping as a basis for selectivity in cadherin adhesion: A mechanism for achieving high specificity and low affinity. Proc. Natl. Acad. Sci. USA *102*, 8531–8536.

Duguay, D., Foty, R.A., and Steinberg, M.S. (2003). Cadherin-mediated cell adhesion and tissue segregation: qualitative and quantitative determinants. Dev. Biol. *253*, 309–323.

Espeseth, A., Marnellos, G., and Kintner, C. (1998). The role of F-cadherin in localizing cells during neural tube formation in Xenopus embryos. Development *125*, 301–312.

Foty, R.A., and Steinberg, M.S. (2005). The differential adhesion hypothesis: a direct evaluation. Dev. Biol. *278*, 255–263.

Hamburger, V., and Hamilton, H.L. (1951). A series of normal stages in the development of the chick embryo. J. Morphol. *88*, 49–92.

Harrison, O.J., Corps, E.M., Berge, T., and Kilshaw, P.J. (2005). The mechanism of cell adhesion by classical cadherins: the role of domain 1. J. Cell Sci. *118*, 711–721.

Hatta, K., and Takeichi, M. (1986). Expression of N-cadherin adhesion molecules associated with early morphogenetic events in chick development. Nature *320*, 447–449.

Haussinger, D., Ahrens, T., Aberle, T., Engel, J., Stetefeld, J., and Grzesiek, S. (2004). Proteolytic E-cadherin activation followed by solution NMR and X-ray crystallography. EMBO J. *23*, 1699–1708.

He, W., Cowin, P., and Stokes, D.L. (2003). Untangling desmosomal knots with electron tomography. Science *302*, 109–113.

May, C., Doody, J.F., Abdullah, R., Balderes, P., Xu, X., Chen, C.P., Zhu, Z., Shapiro, L., Kussie, P., Hicklin, D.J., et al. (2005). Identification of a transiently exposed VE-cadherin epitope that allows for specific targeting of an antibody to the tumor neovasculature. Blood *105*, 4337–4344.

Nagar, B., Overduin, M., Ikura, M., and Rini, J.M. (1996). Structural basis of calcium-induced E-cadherin rigidification and dimerization. Nature *380*, 360–364.

Nakagawa, S., and Takeichi, M. (1995). Neural crest cell-cell adhesion controlled by sequential and subpopulation-specific expression of novel cadherins. Development *121*, 1321–1332.

Niessen, C.M., and Gumbiner, B.M. (2002). Cadherin-mediated cell sorting not determined by binding or adhesion specificity. J. Cell Biol. *156*, 389–399.

Nishimura, E.K., Yoshida, H., Kunisada, T., and Nishikawa, S.I. (1999). Regulation of E- and P-cadherin expression correlated with melanocyte migration and diversification. Dev. Biol. *215*, 155–166.

Nollet, F., Kools, P., and van Roy, F. (2000). Phylogenetic analysis of the cadherin superfamily allows identification of six major subfamilies besides several solitary members. J. Mol. Biol. *299*, 551–572.

Nose, A., Tsuji, K., and Takeichi, M. (1990). Localization of specificity determining sites in cadherin cell adhesion molecules. Cell *61*, 147–155.

Otwinowski, Z., and Minor, W. (1997). Processing of X-ray diffraction data collected in oscillation mode. Methods Enzymol. *A276*, 307–326.

Overduin, M., Harvey, T.S., Bagby, S., Tong, K.I., Yau, P., Takeichi, M., and Ikura, M. (1995). Solution structure of the epithelial cadherin domain responsible for selective cell adhesion. Science *267*, 386–389.

Patel, S.D., Chen, C.P., Bahna, F., Honig, B., and Shapiro, L. (2003). Cadherin-mediated cell-cell adhesion: sticking together as a family. Curr. Opin. Struct. Biol. *13*, 690–698.

Perret, E., Leung, A., Feracci, H., and Evans, E. (2004). Trans-bonded pairs of E-cadherin exhibit a remarkable hierarchy of mechanical strengths. Proc. Natl. Acad. Sci. USA *101*, 16472–16477.

Pertz, O., Bozic, D., Koch, A.W., Fauser, C., Brancaccio, A., and Engel, J. (1999). A new crystal structure, Ca2+ dependence and mutational analysis reveal molecular details of E-cadherin homoassociation. EMBO J. *18*, 1738–1747.

Price, S.R., De Marco Garcia, N.V., Ranscht, B., and Jessell, T.M. (2002). Regulation of motor neuron pool sorting by differential expression of type II cadherins. Cell *109*, 205–216.

Redies, C., and Takeichi, M. (1996). Cadherins in the developing central nervous system: an adhesive code for segmental and functional subdivisions. Dev. Biol. *180*, 413–423.

Redies, C., Treubert-Zimmermann, U., and Luo, J. (2003). Cadherins as regulators for the emergence of neural nets from embryonic divisions. J. Physiol. (Paris) *97*, 5–15.

Shan, W., Yagita, Y., Wang, Z., Koch, A., Svenningsen, A.F., Gruzglin, E., Pedraza, L., and Colman, D.R. (2004). The minimal essential unit for cadherin-mediated intercellular adhesion comprises extracellular domains 1 and 2. J. Biol. Chem. *279*, 55914–55923.

Shan, W.S., Koch, A., Murray, J., Colman, D.R., and Shapiro, L. (1999). The adhesive binding site of cadherins revisited. Biophys. Chem. *82*, 157–163.

Shan, W.S., Tanaka, H., Phillips, G.R., Arndt, K., Yoshida, M., Colman, D.R., and Shapiro, L. (2000). Functional cis-heterodimers of N- and R-cadherins. J. Cell Biol. *148*, 579–590.

Shapiro, L., Fannon, A.M., Kwong, P.D., Thompson, A., Lehmann, M.S., Grubel, G., Legrand, J.F., Als-Nielsen, J., Colman, D.R., and Hendrickson, W.A. (1995a). Structural basis of cell-cell adhesion by cadherins. Nature *374*, 327–337.

Shapiro, L., Kwong, P.D., Fannon, A.M., Colman, D.R., and Hendrickson, W.A. (1995b). Considerations on the folding topology and evolutionary origin of cadherin domains. Proc. Natl. Acad. Sci. USA *92*, 6793–6797.

Shimoyama, Y., Takeda, H., Yoshihara, S., Kitajima, M., and Hirohashi, S. (1999). Biochemical characterization and functional analysis of two type II classic cadherins, cadherin-6 and -14, and comparison with E-cadherin. J. Biol. Chem. *274*, 11987–11994.

Shimoyama, Y., Tsujimoto, G., Kitajima, M., and Natori, M. (2000). Identification of three human type-II classic cadherins and frequent heterophilic interactions between different subclasses of type-II classic cadherins. Biochem. J. *349*, 159–167.

Sivasankar, S., Brieher, W., Lavrik, N., Gumbiner, B., and Leckband, D. (1999). Direct molecular force measurements of multiple adhesive interactions between cadherin ectodomains. Proc. Natl. Acad. Sci. USA *96*, 11820–11824.

Su, X.D., Gastinel, L.N., Vaughn, D.E., Faye, I., Poon, P., and Bjorkman, P.J. (1998). Crystal structure of hemolin: a horseshoe shape with implications for homophilic adhesion. Science *281*, 991–995.

Takeichi, M., Atsumi, T., Yoshida, C., Uno, K., and Okada, T.S. (1981). Selective adhesion of embryonal carcinoma cells and differentiated cells by Ca2+-dependent sites. Dev. Biol. *87*, 340–350.

Tamura, K., Shan, W.S., Hendrickson, W.A., Colman, D.R., and Shapiro, L. (1998). Structure-function analysis of cell adhesion by neural (N-) cadherin. Neuron *20*, 1153–1163.

Tanaka, Y., Nakanishi, H., Kakunaga, S., Okabe, N., Kawakatsu, T., Shimizu, K., and Takai, Y. (2003). Role of nectin in formation of E-cadherin-based adherens junctions in keratinocytes: analysis with the N-cadherin dominant negative mutant. Mol. Biol. Cell *14*, 1597–1609.

Troyanovsky, R.B., Sokolov, E., and Troyanovsky, S.M. (2003). Adhesive and lateral E-cadherin dimers are mediated by the same interface. Mol. Cell. Biol. *23*, 7965–7972.

Troyanovsky, S. (2005). Cadherin dimers in cell-cell adhesion. Eur. J. Cell Biol. *84*, 225–233.

Zhu, B., Chappuis-Flament, S., Wong, E., Jensen, I.E., Gumbiner, B.M., and Leckband, D. (2003). Functional analysis of the structural basis of homophilic cadherin adhesion. Biophys. J. *84*, 4033–4042.

Accession Numbers

The structures reported herein have been deposited in the Protein Data Bank under ID codes 1ZVN, 1ZXK, 2A4C, 2A4E, and 2A62.